Contact Modes and Complementary Cones

Stephen Berard
Department of Computer Science
Rensselaer Polytechnic Institute
Troy, NY 12180
Email: sberard@cs.rpi.edu

Kevin Egan
Department of Computer Science
Rensselaer Polytechnic Institute
Troy, NY 12180
Email: ktegan@cs.rpi.edu

J.C. Trinkle
Department of Computer Science
Rensselaer Polytechnic Institute
Troy, NY 12180
Email: trink@cs.rpi.edu

***Abstract*— In this paper, we use a linear complementarity problem (LCP) formulation of rigid body dynamics with unilateral contacts to obtain definitions for contact modes. We show how the complementary cones of the LCP correspond to each of the intuitive contact modes: *slide right, slide left, roll,* and *separate*. These complementary cones allow us to make rigorous definitions for contact modes in three-dimensional systems, where our intuitive understanding fails.**

I. Introduction

The class of robotic tasks that today are perhaps the most difficult to plan and execute, are those involving intermittent contact. Even when the mathematical model of the robotic system is assumed to be completely known, planning manipulation tasks is quite challenging. One of the problems is the difficulty in determining the sets of wrenches (forces and moments) that should be applied to maintain or achieve certain desirable arrangements of contacts. Typically, to reduce overall complexity, a rigid body model is used [1], [2], [3]. The unfortunate drawback of such models is that they are known to suffer from solution nonuniqueness [4], [5].

In recent work, despite the nonuniqueness problem, Balkcom and Trinkle [6] developed a method for computing the set of all wrenches guaranteed to achieve a particular contact state for planar parts. This approach was based on the common intuitive notion of a contact mode, which, roughly speaking, is a qualitative description of the interactions at a set of contacts. The problem with the intuitive development is that it does not easily extend to three-dimensional systems. In the plane, possible interactions at a contact are *slide left*, *slide right*, *roll*, and *separate*. However for a contact in a three-dimensional space, there is an infinite number of directions that a contact could slide.

In this paper, we use a linear complementarity problem (LCP) formulation of rigid body dynamics to motivate definitions of contact modes; each mode corresponds to a complementary cone [7] of the LCP. We also show the equivalence between the intuitively motivated contact modes and those implied directly by the LCP. This then makes clear how contact modes should be defined for three-dimensional systems, which is done at the end of the paper.

II. Dynamic Model in the Plane

The dynamic model of a workpiece interacting with a number of objects (the three small circles) permanently at rest is shown in Figure 1 and is composed of the four pieces described below.

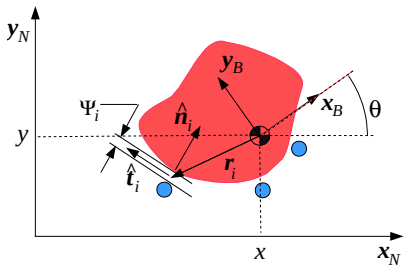

Fig. 1. The dynamic model of a workpiece with three stationary objects

1) Newton-Euler Equations: Let $c_{i\mathrm{n}}$ and $c_{i\mathrm{t}}$ be the normal and tangential components of the contact force applied by stationary object i to the workpiece. Collecting all the normal and tangential components into the vectors $\boldsymbol{c}_{\mathrm{n}} = [\ldots c_{i\mathrm{n}} \ldots]^T$ and $\boldsymbol{c}_{\mathrm{t}} = [\ldots c_{i\mathrm{t}} \ldots]^T$, the Newton-Euler equations can be written as follows:

$$\boldsymbol{M}\dot{\boldsymbol{\nu}} = \boldsymbol{W}_{\mathrm{n}}\boldsymbol{c}_{\mathrm{n}} + \boldsymbol{W}_{\mathrm{t}}\boldsymbol{c}_{\mathrm{t}} + \boldsymbol{w}_{\mathrm{ext}} + \boldsymbol{h} \quad (1)$$

$$\dot{\boldsymbol{q}} = \boldsymbol{G}\boldsymbol{\nu} \quad (2)$$

where $\boldsymbol{M} = diag(m,\ m,\ J)$, $\boldsymbol{w}_{\mathrm{ext}} = [f_x\ f_y\ \tau_z]^T$ is the external wrench (force and moment) applied to the workpiece, $\boldsymbol{G}$ is a Jacobian matrix that allows for different parameterizations of $SO(3)$, $\boldsymbol{W}_{\mathrm{n}}$ and $\boldsymbol{W}_{\mathrm{t}}$ are Jacobian matrices (also called "wrench matrices") that map the contact forces to their equivalent wrenches in the body-fixed frame, and $\boldsymbol{h}$ is a vector containing the velocity product terms. The columns of these matrices are the unit wrenches associated with each of the stationary objects. The complete definitions are:

$$\boldsymbol{W}_{\mathrm{n}} = \begin{bmatrix} \cdots & \hat{\boldsymbol{n}}_i & \cdots \\ & \boldsymbol{r}_i \otimes \hat{\boldsymbol{n}}_i & \end{bmatrix} \quad \boldsymbol{W}_{\mathrm{t}} = \begin{bmatrix} \cdots & \hat{\boldsymbol{t}}_i & \cdots \\ & \boldsymbol{r}_i \otimes \hat{\boldsymbol{t}}_i & \end{bmatrix} \quad (3)$$

where $\boldsymbol{r}_i \otimes \hat{\boldsymbol{n}}_i$ is defined as $r_{i\mathrm{x}} n_{i\mathrm{y}} - r_{i\mathrm{y}} n_{i\mathrm{x}}$ and $r_{i\mathrm{x}}$, $r_{i\mathrm{y}}$, $n_{i\mathrm{x}}$, and $n_{i\mathrm{y}}$ are the x- and y-components of $\boldsymbol{r}_i$ and $\hat{\boldsymbol{n}}_i$, respectively.

2) Kinematic Equations: Let $\boldsymbol{\Psi}(\boldsymbol{q}) = [\ldots \Psi_i(\boldsymbol{q}) \ldots]^T$ be the vector of distances between the workpiece and all the stationary objects. The first and second time derivatives of $\Psi_i(\boldsymbol{q})$ are the normal components of the relative velocity $v_{i\mathrm{n}}$ and acceleration $a_{i\mathrm{n}}$ between the workpiece and object i. Defining the normal velocity and acceleration vectors $\boldsymbol{v}_{\mathrm{n}} = [\ldots v_{i\mathrm{n}} \ldots]^T$ and $\boldsymbol{a}_{\mathrm{n}} = [\ldots a_{i\mathrm{n}} \ldots]^T$, allows one to write the

velocity and acceleration relationships at all the objects in the following form:

$$\boldsymbol{v}_{\mathrm{n}} = \boldsymbol{W}_{\mathrm{n}}{}^{T}\boldsymbol{\nu}, \quad (4)$$

$$\boldsymbol{a}_{\mathrm{n}} = \boldsymbol{W}_{\mathrm{n}}{}^{T}\dot{\boldsymbol{\nu}} + \dot{\boldsymbol{W}}_{\mathrm{n}}{}^{T}\boldsymbol{\nu}. \quad (5)$$

Note that $\boldsymbol{W}_{\mathrm{n}}{}^{T} = \nabla_q \boldsymbol{\Psi}$, where ∇_q denotes the partial derivative with respect to the elements of the vector $\boldsymbol{q}$. Analogous tangential kinematic equations that will be needed are:

$$\boldsymbol{v}_{\mathrm{t}} = \boldsymbol{W}_{\mathrm{t}}{}^{T}\boldsymbol{\nu} \quad (6)$$

$$\boldsymbol{a}_{\mathrm{t}} = \boldsymbol{W}_{\mathrm{t}}{}^{T}\dot{\boldsymbol{\nu}} + \dot{\boldsymbol{W}}_{\mathrm{t}}{}^{T}\boldsymbol{\nu}. \quad (7)$$

3) Normal Complementarity: The normal complementarity constraint, arises from the fundamental observed phenomenon that contact must exist in order for there to be a nonzero contact force. That is, the solution to the dynamic model may have $c_{i\mathrm{n}} > 0$ if and only if $a_{i\mathrm{n}} = 0$. Conversely, if a contact is breaking, then $a_{i\mathrm{n}} > 0$ and $c_{i\mathrm{n}} = 0$. These constraints can be written concisely for all contacts as follows:

$$0 \leq \boldsymbol{a}_{\mathrm{n}} \perp \boldsymbol{c}_{\mathrm{n}} \geq 0, \quad (8)$$

where the symbol $\perp$ indicates normality, (*i.e.*, $\boldsymbol{a}_{\mathrm{n}}^{T}\boldsymbol{c}_{\mathrm{n}} = 0$).

4) Friction Law: It is assumed that Coulomb friction acts at the contacts. Coulomb's law states that at a rolling contact the contact force lies within a cone of possible contact forces. By contrast, at a sliding contact, the contact force must lie on the boundary of a cone in the direction maximizing the dissipation of energy. Coulomb's law can be written as follows:

$$|c_{it}| \leq \mu_{is} c_{i\mathrm{n}} \qquad i \in \mathcal{R} \quad (9)$$

$$c_{it} = -sign(v_{it})\mu_{i\mathrm{k}} c_{i\mathrm{n}} \qquad i \in \mathcal{S} \quad (10)$$

where $\mathcal{R} = \{i \mid \Psi_i = v_{i\mathrm{n}} = v_{it} = 0\}$ is the index set identifying rolling contacts, $\mathcal{S} = \{i \mid \Psi_i = v_{i\mathrm{n}} = 0;\ v_{it} \neq 0\}$ is the index set identifying the sliding contacts, and μ_{is} and $\mu_{i\mathrm{k}}$ are the static and kinetic coefficients of friction at contact i.

In the discussion of instantaneous contact modes to follow, it will be convenient to manipulate the equations above into a more concise form. First, let $\mathcal{J} = \begin{bmatrix} \boldsymbol{W}_{\mathrm{n}} & \boldsymbol{W}_{\mathrm{t}} \end{bmatrix}$ denote the constraint Jacobian matrix. Solving equation (1) for $\dot{\boldsymbol{\nu}}$ and substituting into equations (5) and (7) yields a linear relationship between the contact accelerations and contact forces:

$$\boldsymbol{a} = \boldsymbol{A}\boldsymbol{c} + \boldsymbol{B}\boldsymbol{w}_{\mathrm{ext}} + \boldsymbol{h}, \quad (11)$$

where $\boldsymbol{a} = \begin{bmatrix} \boldsymbol{a}_{\mathrm{n}} \\ \boldsymbol{a}_{\mathrm{t}} \end{bmatrix}$, $\boldsymbol{c} = \begin{bmatrix} \boldsymbol{c}_{\mathrm{n}} \\ \boldsymbol{c}_{\mathrm{t}} \end{bmatrix}$, $\boldsymbol{A} = \mathcal{J}^{T}\boldsymbol{M}^{-1}\mathcal{J}$ and $\boldsymbol{B} = \mathcal{J}\boldsymbol{M}^{-1}$. The dynamic model is now given by equations (8,9, 10,11) with auxiliary equations (4,6) needed only to formulate the model.

III. Contact Modes in The Plane

Contact modes are combinations of relative motions at the point of contact. Four possibilities are: separating (s), rolling (n), sliding left (l), or sliding right (r). In addition, in the part seating problem in which contact is not quite initially achieved, it is important to define an additional mode, approach (a), as was done in [8].

General manipulation tasks can be viewed as a sequence of contact modes leading from an initial state to a goal state. However, to successfully execute the sequence and accomplish the task, one must be able to maintain contact modes and effect transitions between them. One approach to this is to compute sets of forces guaranteed (under a dynamic model) to control the contact modes. In order to do this, we should distinguish between the current contact mode and the impending contact mode. For example, given a ball at rest on a horizontal surface, the current contact mode is n. In the next time instant, the mode could be any of l, n, r, or s, but not a.

To help solidify the ideas of contact modes, Figure 2 shows a disc initially at rest and in contact with a small fixed disc. The static friction coefficient at the contact is assumed to be 0.4. The objective is to identify the set of external wrenches that would maintain contact with this disc and achieve contact with the other disc. The arrows are the "generators" of the wrench cone corresponding to mode 'la'. That is, any vector in the cone can be written as a nonnegative linear combination of the generators. The generators are consistent with our expectations. Specifically, if a force is applied along the generator on the edge of the friction cone, then the disc will not move. However, if this force is augmented by even the slightest application of forces along either or both of the other generators, then the disc will slip downward while the gap at disc 2 is reduced.

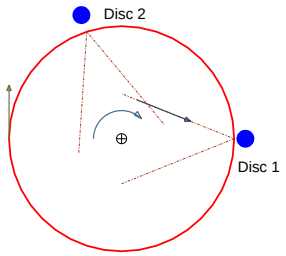

Fig. 2. mode 'la': slide left-approach

Tables I and II show the possible contact modes for a single contact and their relationships to the unknowns of the instantaneous model given above.

Given n existing contacts, there are 4^n potential contact modes, of which only a fraction are kinematically feasible [9]. The set of external wrenches consistent with each mode is a convex set obtained by setting various quantities to zero and then removing them from the model. For example, if one desires the set of external wrenches consistent with maintaining rolling contact at contact i, then one sets $a_{i\mathrm{n}}$ and a_{it} to zero, constrains $c_{i\mathrm{n}}$ to be nonnegative, and requires c_{it} to satisfy equation (9). Any other constraints, such as the complementarity constraint between $a_{i\mathrm{n}}$ and $c_{i\mathrm{n}}$ equation (8), become redundant. If similar assumptions are made for all the contacts, the dynamic model (11) reduces to a system of linear equations and inequalities, which in general defines a polytope in the space of contact forces and accelerations.

Interaction	Abbreviation	a_{in}	a_{it}	c_{in}	c_{it}
separate	s	> 0	–	$= 0$	$= 0$
slide left	l	$= 0$	> 0	> 0	$= -\mu_{ik}\, c_{in}$
roll	n	$= 0$	$= 0$	> 0	$\lvert c_{it}\rvert \leq \mu_{is}\, c_{in}$
slide right	r	$= 0$	< 0	> 0	$= \mu_{ik}\, c_{in}$

TABLE I

INTUITIVE CONTACT MODES FOR AN OBJECT INITIALLY IN CONTACT

Interaction	Abbreviation	a_{in}	a_{it}	c_{in}	c_{it}
separate	s	> 0	–	$= 0$	$= 0$
approach	a	< 0	–	$= 0$	$= 0$

TABLE II

INTUITIVE CONTACT MODES FOR AN OBJECT INITIALLY SEPARATED

If we assume that $\boldsymbol{h}$ in equation (11) is negligible (it is zero in the planar case), then we can rewrite the equation as follows:

$$\boldsymbol{K} \begin{bmatrix} \boldsymbol{a} \\ \boldsymbol{c} \end{bmatrix} = \boldsymbol{P}\boldsymbol{w}_{ext} \tag{12}$$

$$\begin{bmatrix} \boldsymbol{a} \\ \boldsymbol{c} \end{bmatrix} \geq 0 \tag{13}$$

where $\boldsymbol{K} = [\boldsymbol{I}_{2n\times 2n} \; -\boldsymbol{A}]$. Now the polytope defined earlier becomes a convex polyhedral cone, which can be expressed as a system of linear inequalities in the following two equivalent forms:

$$\text{polar}(\boldsymbol{F}) = \{\boldsymbol{w}_{ext} : \boldsymbol{F}\boldsymbol{w}_{ext} \leq 0\} \tag{14}$$

$$\text{pos}(\boldsymbol{G}) = \{\boldsymbol{w}_{ext} : \boldsymbol{w}_{ext} = \boldsymbol{G}\boldsymbol{z} \text{ for some } \boldsymbol{z} \geq 0\} \tag{15}$$

Note that $\boldsymbol{F}$ can be computed from $\boldsymbol{K}$ and $\boldsymbol{P}$ by a moderately complicated procedure given in [6]. However, reformulating equations (8,9,10,11) as a linear complementarity problem will reveal a very simple way to obtain the matrix $\boldsymbol{G}$.

Before proceeding, it is worth making a few comments about the forms of the cone given in equations (14) and (15). Figure 3 gives an example of a cone with both representations shown. Since every $\boldsymbol{w}_{ext} \in \text{polar}(\boldsymbol{F})$ makes a non-positive dot product with each row of $\boldsymbol{F}$, the rows of $\boldsymbol{F}$ can be interpreted as outward facing normal vectors to the facets of the polyhedral cone. The cone can be seen then as the intersection of half-spaces and thus has its apex at the origin. This form is referred to as "face form." In the second form, the columns of $\boldsymbol{G}$ play the roll of generators of the cone. This form is referred to as "span form." Conversion between these forms can be accomplished in general by linear programming methods [10].

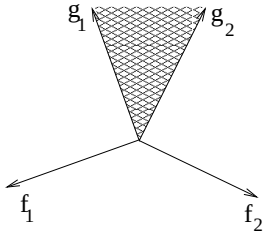

Fig. 3. Face and Span representations of a polyhedral convex cone. f_i is the ith row of F (Face form) while g_i is the ith column of G (Span form)

IV. FORMULATION OF THE MODEL AS AN LCP

The standard linear complementarity problem [7], can be stated as follows:

*Definition 1 (**LCP($\boldsymbol{B}$, $\boldsymbol{b}$)**):* Given the constant matrix $\boldsymbol{B} \in \Re^{m\times m}$ and vector $\boldsymbol{b} \in \Re^m$, find vectors $\boldsymbol{z} \in \Re^m$, $\boldsymbol{y} \in \Re^m$ satisfying the following conditions:

$$\boldsymbol{y} = \boldsymbol{B}\boldsymbol{z} + \boldsymbol{b} \tag{16}$$

$$0 \leq \boldsymbol{y} \perp \boldsymbol{z} \geq 0 \tag{17}$$

This LCP is said to be of size m.

In [11], the instantaneous dynamic model was manipulated obtaining an LCP for spatial bodies in contact. Below we have specialized this formulation for two dimensional systems.

This is done by eliminating c_{it} for all sliding contacts and changing force and acceleration variables at all rolling contacts. Let us rewrite the tangential acceleration at contact $i \in \mathcal{R}$ as the sum of its positive and negative parts (*i.e.*, $a_{it} = a_{it}^+ - a_{it}^-$, where $a_{it}^+, a_{it}^- \geq 0$). Denoting the vector of tangential accelerations at all the rolling contacts as $\boldsymbol{a}_{\mathcal{R}\text{t}} = [\ldots a_{it} \ldots]^T \; \forall \; i \in \mathcal{R}$, and similarly defining the positive and negative parts, $\boldsymbol{a}_{\mathcal{R}\text{t}}^+$ and $\boldsymbol{a}_{\mathcal{R}\text{t}}^-$, we have:

$$\boldsymbol{a}_{\mathcal{R}\text{t}} = \boldsymbol{a}_{\mathcal{R}\text{t}}^+ - \boldsymbol{a}_{\mathcal{R}\text{t}}^-. \tag{18}$$

We also define complementary slack variables $s_{it}^+ = \mu_{is}c_{in} + c_{it}$ and $s_{it}^- = \mu_{is}c_{in} - c_{it}$ and $s_{it}^+, s_{it}^- \geq 0$ for $i \in \mathcal{R}$.[1] In matrix form, the slack conditions for all the rolling contacts are:

$$\boldsymbol{s}_{\mathcal{R}\text{t}}^+ = \boldsymbol{U}_{\mathcal{R}}\boldsymbol{c}_{\mathcal{R}\text{n}} + \boldsymbol{c}_{\mathcal{R}\text{t}} \tag{19}$$

$$\boldsymbol{s}_{\mathcal{R}\text{t}}^- = \boldsymbol{U}_{\mathcal{R}}\boldsymbol{c}_{\mathcal{R}\text{n}} - \boldsymbol{c}_{\mathcal{R}\text{t}}, \tag{20}$$

where $\boldsymbol{s}_{\mathcal{R}\text{t}}^+$ and $\boldsymbol{s}_{\mathcal{R}\text{t}}^-$ are defined analogously to $\boldsymbol{a}_{\mathcal{R}\text{t}}^+$ and $\boldsymbol{a}_{\mathcal{R}\text{t}}^-$ above and $\boldsymbol{U}_{\mathcal{R}}$ is the diagonal matrix with diagonal elements equal to the coefficients of static friction at the rolling contacts.

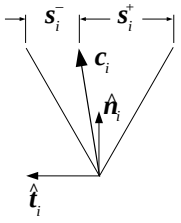

Fig. 4. Slack variables are interpreted as the distance between the tip of a contact force c_{in} and the edge of its friction cone. Leftward sliding ($a_{it}^+ > 0$) implies that the right side slack ($s_{it}^+ = 0$), and therefore, the left side slack is maximized ($s_{it}^- = 2\mu_{is}c_{in}$).

[1] Even though the contact can begin sliding at the instant the instantaneous model is solved, we assume the static coefficient of friction applies. In a simulation setting, after sliding begins, then the kinetic coefficient applies through equation (10).

The above definitions lead to the following tangential complementarity constraints at the rolling contacts:

$$0 \leq \boldsymbol{a}^+_{\mathcal{R}\mathrm{t}} \quad \perp \quad \boldsymbol{s}^+_{\mathcal{R}\mathrm{t}} \geq 0 \tag{21}$$

$$0 \leq \boldsymbol{a}^-_{\mathcal{R}\mathrm{t}} \quad \perp \quad \boldsymbol{s}^-_{\mathcal{R}\mathrm{t}} \geq 0. \tag{22}$$

Notice that when $a^+_{i\mathrm{t}}$ is positive (leftward sliding), then $s^+_{i\mathrm{t}}$ must equal zero, which implies that the contact force lies on the right edge of the friction cone as required. Conversely, when $s^+_{i\mathrm{t}}$ is positive the contact force lies to the left of the right edge of the cone implying that leftward acceleration is impossible (*i.e.,* $a^+_{i\mathrm{t}} = 0$). The analogous statements hold for $a^-_{i\mathrm{t}}$ and $s^-_{i\mathrm{t}}$.

Using equation (10) to eliminate $c_{i\mathrm{t}}$ for all $i \in \mathcal{S}$, combining equations (1,5,7,18,19,20), and appending equations (8,21,22), we arrive at the following LCP formulation of the instantaneous dynamic model:

$$\begin{bmatrix} \boldsymbol{a}_{\mathcal{S}\mathrm{n}} \\ \boldsymbol{a}_{\mathcal{R}\mathrm{n}} \\ \boldsymbol{a}^+_{\mathcal{R}\mathrm{t}} \\ \boldsymbol{s}^-_{\mathcal{R}\mathrm{t}} \end{bmatrix} = \boldsymbol{B} \begin{bmatrix} \boldsymbol{c}_{\mathcal{S}\mathrm{n}} \\ \boldsymbol{c}_{\mathcal{R}\mathrm{n}} \\ \boldsymbol{s}^+_{\mathcal{R}\mathrm{t}} \\ \boldsymbol{a}^-_{\mathcal{R}\mathrm{t}} \end{bmatrix} + \boldsymbol{b} \tag{23}$$

$$\boldsymbol{a}_{\mathcal{S}\mathrm{n}},\, \boldsymbol{c}_{\mathcal{S}\mathrm{n}},\, \boldsymbol{a}_{\mathcal{R}\mathrm{n}},\, \boldsymbol{c}_{n\mathcal{R}},\, \boldsymbol{a}^+_{\mathcal{R}\mathrm{t}},\, \boldsymbol{s}^+_{\mathcal{R}\mathrm{t}},\, \boldsymbol{a}^-_{\mathcal{R}\mathrm{t}},\, \boldsymbol{s}^-_{\mathcal{R}\mathrm{t}} \geq 0 \tag{24}$$

$$\boldsymbol{a}^T_{\mathcal{S}\mathrm{n}}\boldsymbol{c}_{\mathcal{S}\mathrm{n}} = \boldsymbol{a}^T_{\mathcal{R}\mathrm{n}}\boldsymbol{c}_{n\mathcal{R}} = (\boldsymbol{a}^+_{\mathcal{R}\mathrm{t}})^T\boldsymbol{s}^+_{\mathcal{R}\mathrm{t}} = (\boldsymbol{a}^-_{\mathcal{R}\mathrm{t}})^T\boldsymbol{s}^-_{\mathcal{R}\mathrm{t}} = 0 \tag{25}$$

where the values of $\boldsymbol{B}$ and $\boldsymbol{b}$ can be found in [11] but are not required in our analysis.

V. LCP-Motivated Contact Modes in the Plane

For a given contact state, one can compute a polyhedral cone of external wrenches consistent with each contact mode defined intuitively earlier. An LCP of size n implicitly defines 2^n n-dimensional convex polyhedral cones that arise as follows. Equation (23) is rewritten with $y = [\boldsymbol{a}_{\mathcal{S}\mathrm{n}}\ \boldsymbol{a}_{\mathcal{R}\mathrm{n}}\ \boldsymbol{a}^+_{\mathcal{R}\mathrm{t}}\ \boldsymbol{s}^-_{\mathcal{R}\mathrm{t}}]^T$ and $z = [\boldsymbol{c}_{\mathcal{S}\mathrm{n}}\ \boldsymbol{c}_{\mathcal{R}\mathrm{n}}\ \boldsymbol{s}^+_{\mathcal{R}\mathrm{t}}\boldsymbol{a}^-_{\mathcal{R}\mathrm{t}}]^T$ on the same side:

$$[\boldsymbol{I} \quad -\boldsymbol{B}] \begin{bmatrix} \boldsymbol{y} \\ \boldsymbol{z} \end{bmatrix} = \boldsymbol{b} \tag{26}$$

$$0 \leq \boldsymbol{y} \perp \boldsymbol{z} \geq 0. \tag{27}$$

Let $\mathcal{I} \subseteq \{1, ..., n\}$ and its complement $\overline{\mathcal{I}}$ over $\{1, ..., n\}$ denote two index sets. An n-dimensional complementary cone is then defined by choosing complementary elements of $\boldsymbol{y}$ and $\boldsymbol{z}$ to be strictly positive, (*i.e.,* $\boldsymbol{y}_{\mathcal{I}}, \boldsymbol{z}_{\overline{\mathcal{I}}} > 0$). Having done this, equation (27) requires that $\boldsymbol{y}_{\overline{\mathcal{I}}} = 0$ and $\boldsymbol{z}_{\mathcal{I}} = 0$, and so these unknowns may be removed from equations (26) and (27) to directly yield the following span form representation of a convex polyhedral cone:

$$\boldsymbol{G}\boldsymbol{\xi} \;=\; \boldsymbol{b} \tag{28}$$

$$\boldsymbol{\xi} \;>\; 0, \tag{29}$$

where $\boldsymbol{G} \in \Re^{n \times n}$. Note that n is the maximum number of positive elements out of the $2n$ elements of $\boldsymbol{y}$ and $\boldsymbol{z}$. Choosing more than n elements to be zero is physically allowable, but degenerate and will not be considered here.

A. Equivalence Between LCP-Formulated and Intuitively-Motivated Contact Modes

In this section, we show that the intuitively-motivated contact modes are identical to those obtained by the LCP formulation and that no other contact modes are possible. We will only consider the cases in which complementarity is satisfied strictly (all variables not set to zero are strictly positive). The degenerate cases simply lie on the boundaries of the non-degenerate sets. Physically they correspond to situations such as rolling with $c_{i\mathrm{n}} = 0$.

Consider the possible contact modes for the i^{th} contact. If the contact is originally sliding, it contributes only two unknowns, $a_{i\mathrm{n}}$ and $c_{i\mathrm{n}}$, to the LCP defined by equations (23-25). Since the only complementary pair of variables is $c_{i\mathrm{n}}$ and $a_{i\mathrm{n}}$ only two contact modes are possible for a single sliding contact:

A) Contact Maintenance ($a_{i\mathrm{n}} = 0,\ c_{i\mathrm{n}} > 0$)

B) Contact Separation ($a_{i\mathrm{n}} > 0,\ c_{i\mathrm{n}} = 0$).

While the transition from sliding to rolling can also occur, this transition is not part of the solution of the LCP. Rather, it is determined in a simulation setting by monitoring the relative sliding speed and designating the contact as a rolling contact once a minimum speed is reached.

When i is originally rolling, three pairs of complementary variables are contributed: $a_{i\mathrm{n}}$ and $c_{i\mathrm{n}}$, $a^+_{i\mathrm{t}}$ and $s^+_{i\mathrm{t}}$, and $a^-_{i\mathrm{t}}$ and $s^-_{i\mathrm{t}}$. Since there are $2^3 = 8$ ways to choose complementary pairs at a rolling contact, one wonders how these relate to the four contact modes, separate, slide left, roll, and slide right, discussed earlier (table I) for rolling contacts. We will now show that four of the eight modes are infeasible and that the four feasible modes are identical to the definitions.

A) Contact Maintenance ($a_{i\mathrm{n}} = 0,\ c_{i\mathrm{n}} > 0$)

1) **Rolling** ($a^+_{i\mathrm{t}} = a^-_{i\mathrm{t}} = 0,\ s^+_{i\mathrm{t}},\ s^-_{i\mathrm{t}} > 0$): This contact mode is feasible and is identified as *rolling* as follows. Since $a^+_{i\mathrm{t}}$ and $a^-_{i\mathrm{t}}$ are zero, strict complementarity constrains $s^+_{i\mathrm{t}}$ and $s^-_{i\mathrm{t}}$ to be positive. This implies that the contact force $\boldsymbol{c}_i$ lies within the friction cone as required by the Coulomb model of friction for rolling contact.
2) **Sliding Left** ($a^-_{i\mathrm{t}} = s^+_{i\mathrm{t}} = 0,\ a^+_{i\mathrm{t}},\ s^-_{i\mathrm{t}} > 0$): This contact mode is feasible and is identified as *leftward sliding* as follows. Since $a^-_{i\mathrm{t}}$ is zero and $a^+_{i\mathrm{t}}$ positive, the motion at the contact is leftward. Since $s^+_{i\mathrm{t}}$ is zero, the contact force $\boldsymbol{c}_i$ must lie on the right edge of the friction cone as required by Coulomb's law, which is also consistent with $s^-_{i\mathrm{t}}$ nonnegative.
3) **Sliding Right** ($a^+_{i\mathrm{t}} = s^-_{i\mathrm{t}} = 0,\ a^-_{i\mathrm{t}},\ s^+_{i\mathrm{t}} > 0$): Analysis is identical to sliding left after exchanging + and - superscripts.
4) Infeasible ($a^+_{i\mathrm{t}},\ a^-_{i\mathrm{t}} > 0,\ s^+_{i\mathrm{t}} = s^-_{i\mathrm{t}} = 0$): This contact mode is physically infeasible, since $a^+_{i\mathrm{t}} > 0$ and $a^-_{i\mathrm{t}} > 0$ mean that the contact is simultaneously sliding leftward and rightward. Also, since $c_{i\mathrm{n}} > 0$, both $s^+_{i\mathrm{t}}$ and $s^-_{i\mathrm{t}}$ cannot be 0 simultaneously (see Figure 4).

B) Contact Separation ($a_{i\mathrm{n}} > 0,\ c_{i\mathrm{n}} = 0$)

Since $c_{i\mathrm{n}} = 0$, equations (9) and (10) require $c_{i\mathrm{t}}$ to be zero,

which requires s_{it}^+ and s_{it}^- to be zero.

1) Infeasible ($s_{it}^+,\ s_{it}^- > 0,\ a_{it}^+ = a_{it}^- = 0$): Both s_{it}^+ and s_{it}^- must be zero.
2) Infeasible ($a_{it}^+,\ s_{it}^- > 0,\ s_{it}^+ = a_{it}^- = 0$): s_{it}^- is positive.
3) Infeasible ($a_{it}^-,\ s_{it}^+ > 0,\ s_{it}^- = a_{it}^+ = 0$): s_{it}^+ is positive.
4) **Separation** ($a_{it}^+,\ a_{it}^- > 0,\ s_{it}^+ = s_{it}^- = 0$): s_{it}^+ and s_{it}^- are zero as needed and the positivity of a_{it}^+ and a_{it}^- imply that the tangential acceleration at the contact is unconstrained, as one would expect.

In the intuitive analysis we defined the contact mode approach (**a**) which is possible when there is no contact. In the LCP-formulation, approach can be analyzed by assuming contact exists, and then changing the sign of $a_{i\mathrm{n}}$ by a simple change of variables. Once done, this case is identical to the case of separation, since s_{it}^+ and s_{it}^- must be zero. Therefore, we know that only the fourth choice is feasible.

C) Contact Approach ($-a_{i\mathrm{n}} > 0,\ c_{i\mathrm{n}} = 0$)

1) **Approach** ($a_{it}^+,\ a_{it}^- > 0,\ s_{it}^+ = s_{it}^- = 0$)

The above analysis demonstrates, that the contact modes implied by the LCP formulation are identical to those derived intuitively.

VI. Extending the model into 3-dimensions

The LCP formulation can be easily extended to 3D (see [11] for details):

$$\begin{bmatrix} \boldsymbol{a}_{\mathcal{S}\mathrm{n}} \\ \boldsymbol{a}_{\mathcal{R}\mathrm{n}} \\ \boldsymbol{a}_{\mathcal{R}\mathrm{t}}^+ \\ \boldsymbol{a}_{\mathcal{R}\mathrm{o}}^+ \\ \boldsymbol{s}_{\mathcal{R}\mathrm{t}}^- \\ \boldsymbol{s}_{\mathcal{R}\mathrm{o}}^- \end{bmatrix} = \boldsymbol{B} \begin{bmatrix} \boldsymbol{c}_{\mathcal{S}\mathrm{n}} \\ \boldsymbol{c}_{\mathcal{R}\mathrm{n}} \\ \boldsymbol{s}_{\mathcal{R}\mathrm{t}}^+ \\ \boldsymbol{s}_{\mathcal{R}\mathrm{o}}^+ \\ \boldsymbol{a}_{\mathcal{R}\mathrm{t}}^- \\ \boldsymbol{a}_{\mathcal{R}\mathrm{o}}^- \end{bmatrix} + \boldsymbol{b} \tag{30}$$

$$\boldsymbol{a}_{\mathcal{S}\mathrm{n}}, \boldsymbol{a}_{\mathcal{R}\mathrm{n}}, \boldsymbol{a}_{\mathcal{R}\mathrm{t}}^+, \boldsymbol{a}_{\mathcal{R}\mathrm{t}}^-, \boldsymbol{a}_{\mathcal{R}\mathrm{o}}^+, \boldsymbol{a}_{\mathcal{R}\mathrm{o}}^-, \boldsymbol{c}_{\mathcal{S}\mathrm{n}}, \boldsymbol{c}_{\mathcal{R}\mathrm{n}}, \boldsymbol{s}_{\mathcal{R}\mathrm{t}}^+, \boldsymbol{s}_{\mathcal{R}\mathrm{t}}^-, \boldsymbol{s}_{\mathcal{R}\mathrm{o}}^+, \boldsymbol{s}_{\mathcal{R}\mathrm{o}}^- \geq 0 \tag{31}$$

$$\begin{aligned}(\boldsymbol{a}_{\mathcal{S}\mathrm{n}})^T \boldsymbol{c}_{\mathcal{S}\mathrm{n}} = (\boldsymbol{a}_{\mathcal{R}\mathrm{n}})^T \boldsymbol{c}_{\mathcal{R}\mathrm{n}} = (\boldsymbol{a}_{\mathcal{R}\mathrm{t}}^+)^T \boldsymbol{s}_{\mathcal{R}\mathrm{t}}^+ \\ = (\boldsymbol{a}_{\mathcal{R}\mathrm{o}}^+)^T \boldsymbol{s}_{\mathcal{R}\mathrm{o}}^+ = (\boldsymbol{s}_{\mathcal{R}\mathrm{t}}^-)^T \boldsymbol{a}_{\mathcal{R}\mathrm{t}}^- = (\boldsymbol{s}_{\mathcal{R}\mathrm{o}}^-)^T \boldsymbol{a}_{\mathcal{R}\mathrm{o}}^- = 0\end{aligned} \tag{32}$$

where again the definitions of $\boldsymbol{B}$ and $\boldsymbol{b}$ can be found in [11] and a graphical interpretation of the slack variables is shown in Figure 5. The LCP is of size $5|\mathcal{R}| + |\mathcal{S}|$

A. Three-Dimensional Contact Mode Analysis

Analogous to our previous contact mode analysis, consider the possible contact modes for the i^{th} contact. If the contact is originally sliding, it contributes only two unknowns, $a_{i\mathrm{n}}$ and $c_{i\mathrm{n}}$, to the LCP defined by equations (30-32). Since there is only one complementary pair, only two contact modes are possible for a single sliding contact:

A) Contact Maintenance ($a_{i\mathrm{n}} = 0,\ c_{i\mathrm{n}} > 0$)

B) Contact Separation ($a_{i\mathrm{n}} > 0,\ c_{i\mathrm{n}} = 0$).

Now consider the case where i is originally rolling, five complementary pairs of variables are contributed: $a_{i\mathrm{n}}$ and $c_{i\mathrm{n}}$, a_{it}^+ and s_{it}^+, a_{it}^- and s_{it}^-, $a_{i\mathrm{o}}^+$ and $s_{i\mathrm{o}}^+$, and $a_{i\mathrm{o}}^-$ and $s_{i\mathrm{o}}^-$.

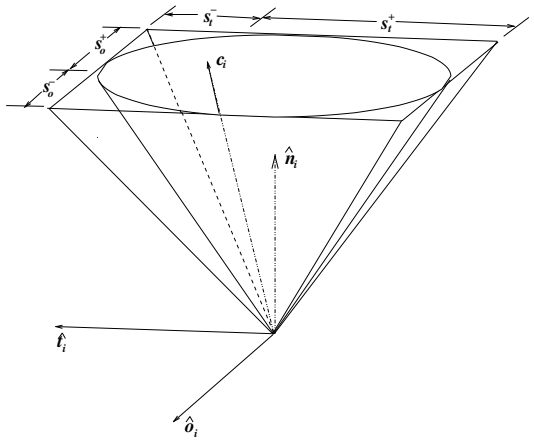

Fig. 5. Rolling contact friction cone with a 4 sided pyramid approximation. Also shown are the slack variables all positive ensuring the contact force c_i lies within the cone.

Therefore, we have $2^5 = 32$ ways to choose complementary pairs at a rolling contact. Using similar arguments as done in the planar analysis we can show that only 10 of these modes are feasible. In order to save space, we will only list the 6 feasible non-degenerate modes. The degenerate modes simply correspond to a transition between sliding direction quadrants. The missing analysis for two of the sliding modes is analogous to one of the sliding modes with the analysis given, and the missing analysis for the infeasible contact modes can be easily verified.

A) Contact Maintenance ($a_{i\mathrm{n}} = 0,\ c_{i\mathrm{n}} > 0$)

1) **Rolling**
($a_{it}^+ = a_{i\mathrm{o}}^+ = a_{it}^- = a_{i\mathrm{o}}^- = 0,\ s_{it}^+,\ s_{i\mathrm{o}}^+,\ s_{it}^-,\ s_{i\mathrm{o}}^- > 0$): This contact mode is feasible and is identified as *rolling* as follows. Since a_{it}^+, $a_{i\mathrm{o}}^+$, a_{it}^-, and $a_{i\mathrm{o}}^-$ are zero, strict complementarity constrains s_{it}^+, $s_{i\mathrm{o}}^+$, s_{it}^-, and $s_{i\mathrm{o}}^-$ to be positive. This implies that the contact force $\boldsymbol{c}_i$ lies within our approximation of the friction cone (as required by the Coulomb model of friction for rolling contact).
2) **Sliding Negative o, Negative t**
($a_{it}^+ = a_{i\mathrm{o}}^+ = s_{it}^- = s_{i\mathrm{o}}^- = 0,\ s_{it}^+,\ s_{i\mathrm{o}}^+,\ a_{it}^-,\ a_{i\mathrm{o}}^- > 0$): Since $a_{it}^+ = 0$, $a_{it}^- > 0$, $a_{i\mathrm{o}}^+ = 0$, and $a_{i\mathrm{o}}^- > 0$ the acceleration direction is somewhere within the $-t$, $-o$ quadrant. Since $s_{it}^- = s_{i\mathrm{o}}^- = 0$ with $s_{it}^+ > 0$ and $s_{i\mathrm{o}}^+ > 0$, the contact force c_i must lie on the vertex of the pyramid in the positive t, positive o quadrant, as required by Coulomb's law.
3) **Sliding Positive o, Negative t**
($a_{it}^+ = s_{i\mathrm{o}}^+ = s_{it}^- = a_{i\mathrm{o}}^- = 0,\ s_{it}^+,\ a_{i\mathrm{o}}^+,\ a_{it}^-,\ s_{i\mathrm{o}}^- > 0$)
4) **Sliding Negative o, Positive t**
($s_{it}^+ = a_{i\mathrm{o}}^+ = a_{it}^- = s_{i\mathrm{o}}^- = 0,\ a_{it}^+,\ s_{i\mathrm{o}}^+,\ s_{it}^-,\ a_{i\mathrm{o}}^- > 0$)
5) **Sliding Positive o, Positive t**
($s_{it}^+ = s_{i\mathrm{o}}^+ = a_{it}^- = a_{i\mathrm{o}}^- = 0,\ a_{it}^+,\ a_{i\mathrm{o}}^+,\ s_{it}^-,\ s_{i\mathrm{o}}^- > 0$)

B) Contact Separation ($a_{i\mathrm{n}} > 0,\ c_{i\mathrm{n}} = 0$):
Since $c_{i\mathrm{n}} = 0$, the formulation requires all the slack variables to be zero. We see that only one mode of the 16 has this requirement. Therefore, there is only one possible separation

mode and all the other modes are infeasible.

1) **Separation**
($s_{it}^{+} = s_{io}^{+} = s_{it}^{-} = s_{io}^{-} = 0,\ a_{it}^{+},\ a_{io}^{+},\ a_{it}^{-},\ a_{io}^{-} > 0$): This is the only contact mode in which all slack variables are zero. We can also see that our frictional accelerations are unconstrained which is expected.

Again, we would like to define the contact mode approach. We know approach is identical to the case of separation if we change the sign of a_{in}. Therefore, there is only one possibility.

C) Contact Approach ($-a_{in} > 0,\ c_{in} = 0$)

1) **Approach**
($s_{it}^{+} = s_{io}^{+} = s_{it}^{-} = s_{io}^{-} = 0,\ a_{it}^{+},\ a_{io}^{+},\ a_{it}^{-},\ a_{io}^{-} > 0$): Identical to separation.

Therefore, this friction model has *Rolling, 4 sliding directions*, *separation*, and *approach* for possible contact modes resulting from the complementary cones of the LCP. Intuitively, we would have expected an infinite number of sliding directions, but in practice this is impossible and the above friction model and resulting LCP formulation gives us the smallest and simplest set of sliding directions.

B. More Accurate Friction Cone Approximation

The 4-sided pyramid approximation of Coulomb's friction cone is a natural extension into 3D; and it is easily converted into a LCP formulation similar to the 2D case. However, a drawback of the 4-sided pyramid approximation is the lack of accuracy (*i.e.* only 4 friction force directions). In this section, we will analyze the possible contact modes using a more accurate friction model developed in [12].

This friction model can be thought of as a k-sided pyramid approximation of the friction cone (see Figure 6). This allows for k (non-degenerate) friction force directions as opposed to the 4 available in the previous model. In order to produce the correct friction force at contact i, the following system of inequalities is used

$$\lambda \boldsymbol{e} + \boldsymbol{a}_f \geq 0 \qquad \boldsymbol{c}_f \geq 0 \tag{33}$$

$$\mu_i c_{in} - \boldsymbol{e}^T \boldsymbol{c}_f \geq 0 \qquad \lambda \geq 0 \tag{34}$$

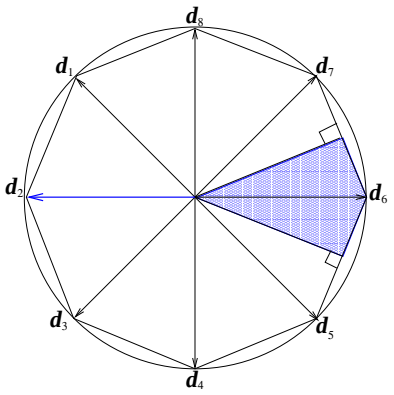

Fig. 6. Overhead view of a sliding contact with the improved friction cone approximation where $k = 8$. Each $\boldsymbol{d}_i$ is one of the spanning vectors in the space of generalized friction forces. Any acceleration in the shaded region corresponds to $c_2 > 0$.

with complimentary conditions:

$$(\lambda \boldsymbol{e} + \boldsymbol{a}_f)\boldsymbol{c}_f = 0 \tag{35}$$

$$(\mu_i c_{in} - \boldsymbol{e}^T \boldsymbol{c}_f)\lambda = 0 \tag{36}$$

where $\boldsymbol{e} = [1, 1, \ldots, 1]^T \in \mathbb{R}^k$ with k being the number of edges of the polyhedral approximation, $\boldsymbol{c}_f \in \mathbb{R}^k$ is a vector of frictional force magnitudes in the k directions, $\boldsymbol{a}_f = \boldsymbol{W}_f^T \dot{\boldsymbol{\nu}} + \dot{\boldsymbol{W}}_f^T \boldsymbol{\nu}$, where $\boldsymbol{a}_f \in \mathbb{R}^k$ is a vector of projections of the tangential acceleration onto the friction directions, and λ is a scalar (explained below). Appending this system of frictional complementarity conditions to the normal complementarity constraints, results in the following complementarity formulation of the dynamic model at contact i:

$$\begin{bmatrix} a_{in} \\ \lambda \boldsymbol{e} + \boldsymbol{a}_{if} \\ \mu_i c_{in} - \boldsymbol{e}^T \boldsymbol{c}_{if} \end{bmatrix} = \boldsymbol{B} \begin{bmatrix} c_{in} \\ \boldsymbol{c}_{if} \\ \lambda \end{bmatrix} + \boldsymbol{b} \tag{37}$$

$$a_n, (\lambda \boldsymbol{e} + \boldsymbol{a}_{if}), (\mu c_n - \boldsymbol{e}^T \boldsymbol{c}_{if}), c_n, \boldsymbol{c}_{if}, \lambda \geq 0 \tag{38}$$

$$(a_n)^T c_n = (\lambda \boldsymbol{e} + \boldsymbol{a}_{if})^T \boldsymbol{c}_{if} = (\mu c_n - \boldsymbol{e}^T \boldsymbol{c}_{if})^T \lambda = 0 \tag{39}$$

where again the definitions of $\boldsymbol{B}$ and $\boldsymbol{b}$ can be found in [12], but are not important for this analysis.

We can then extend this model allowing for multiple contacts as was done in [12]. The multiple contact LCP is of size $|\mathcal{S}| + (k+2)|\mathcal{R}|$.

C. Contact Mode Analysis for Improved Friction Cone Approximation

Since the analysis for a contact originally sliding is identical to above, we will only analyze the case when the contact is originally rolling at a contact i. It contributes k + 2 complimentary pairs. Since there are 2^{k+2} ways to choose complementary pairs, one wonders how these relate to the contact modes discussed earlier. We will now show that only $2k + 4$ ways are feasible, and that the feasible modes relate directly to the modes defined earlier. Since enumeration is impractical, we will take a more logical approach analyzing the system.

A) Contact Maintenance ($a_{in} = 0,\ c_{in} > 0$)

Sliding: In order to make the transition from rolling to sliding, $\|\boldsymbol{a}_{if}\| > 0$. Since the columns of D positively span the space of generalized friction forces, the vector $\boldsymbol{a}_{if}$ contains at least one strictly negative element. Therefore, in order to satisfy the left inequality in (33), λ_i must be positive. Furthermore, it requires $\lambda_i \geq -\min_\xi(a_\xi)$ where $a_\xi \in \boldsymbol{a}_{if}$. Positive λ_i in equation (36) implies the sum of the elements in $\boldsymbol{c}_{if}$ equals $\mu_i c_{in}$. Since $\lambda_i \geq -\min_\xi(a_\xi)$, this implies that the left inequality in (33) will be zero once, twice, or never (the twice and never cases are degenerate and discussed later). Looking at the right inequality, we see the perpendicularity constraint (in strict complementarity) forces the respective element in $\boldsymbol{c}_{if}$ to be positive. Since this element must equal $\mu_i c_{in}$, the contact force must lie on the edge of the friction cone satisfying Coulomb's law for sliding.

One possible set of degenerate cases happens when two elements of $\boldsymbol{c}_{if}$ are positive. This can only happen when two elements of a_ξ equal $-\min_\xi(a_\xi)$. However, even in this situation, the left inequality in (34) still requires the elements of $\boldsymbol{c}_{if}$ to sum to $\mu_i c_{in}$. Therefore, the friction force is constrained to a face of the pyramid.

Usually $\lambda_i = -\min_\xi(a_\xi)$, but if λ_i is $> -\min_\xi(a_\xi)$, we have a degenerate case in which all elements of $\boldsymbol{c}_{if}$ are zero. Equation (36) still must be satisfied, which can only happen if either μ_i is zero and/or c_{in} is zero. Since we assumed $c_{in} > 0$ above, this degenerate case is only possible when $\mu_i = 0$ (*i.e.* no friction).

Using the above analysis, we see the 2^{k+1} possible modes for maintaining contact reduce to $2k+1$ feasible modes for sliding. There are k non-degenerate cases, and $k+1$ degenerate cases (one for each of the k cases where two elements of $\boldsymbol{c}_{if}$ are non-zero, and one for when μ is zero). We will now again only enumerate the non-degenerate feasible modes below using the following: let $c_j \in \boldsymbol{c}_{if}$ and $a_j \in (\lambda_i \boldsymbol{e} + \boldsymbol{a}_{if})$ for some $j = [0, \ldots, k]$

1) **Sliding in $\boldsymbol{a}_{if}$ direction**
$(\boldsymbol{c}_{if} - c_j) = a_j = (\mu_i c_{in} - \boldsymbol{e}^T \boldsymbol{c}_{if}) = 0$
$\lambda_i, c_j, ((\lambda_i \boldsymbol{e} + \boldsymbol{a}_{if}) - a_j) > 0$

Rolling: In order to remain rolling, $\|\boldsymbol{a}_{if}\| = 0$. Looking at the left inequality in (33), this leaves two choices for λ_i: $\lambda_i > 0$ or $\lambda_i = 0$. If $\lambda_i = 0$, then the inequalities in (33) imply $\boldsymbol{c}_{if} > 0$. Using these results in the inequalities defined in (34), we see $(\boldsymbol{e}^T \boldsymbol{c}_{if} < \mu_i c_{in})$. This allows the contact force to range over the interior surface of the k-sided friction cone approximation (as expected in rolling).

The other choice for λ_i is a degenerate case. $\lambda_i > 0$ implies that $\boldsymbol{c}_{if} = 0$. We still must satisfy equation (36), which forces $\mu_i c_{in} = 0$. Analogous to the situation for sliding, this can only happen with the lack of friction (*i.e* $\mu_i = 0$).

Using the above logic, we see the 2^{k+1} total possible modes for maintaining contact reduce to 2 modes for a rolling contact, and we have listed the non-degenerate mode below:

1) **Rolling**
$(\lambda_i \boldsymbol{e} + \boldsymbol{a}_{if}) = \lambda_i = 0$
$(\mu_i c_{in} - \boldsymbol{e}^T \boldsymbol{c}_{if}), \boldsymbol{c}_{if} > 0$

B) Contact Separation ($a_{\mathrm{in}} > 0,\ c_{\mathrm{in}} = 0$)
Separation: $c_{\mathrm{in}} = 0$ implies from the left inequality in (34) that $\boldsymbol{c}_{if} = 0$. Using the inequalities in (34) we see λ must be positive. We also have unconstrained frictional acceleration as one would expect. Therefore, the 2^{k+1} possible modes for contact separation are reduced to 1 possible choice, shown below:

1) **Separation**
$\boldsymbol{c}_{if} = (\mu_i c_{in} - \boldsymbol{e}^T \boldsymbol{c}_{if}) = 0$
$\lambda_i, (\lambda_i \boldsymbol{e} + \boldsymbol{a}_{if}) > 0$

Again, we would like to define the contact mode approach. We know from previous analysis that approach can be analyzed by changing the sign of a_{in} and then this case is identical to the case of separation. Therefore, again to save space, we only list the one feasible mode.

C) Contact Approach

1) **Approach**
$c_{\mathrm{in}} = \boldsymbol{c}_{if} = (\mu_i c_{in} - \boldsymbol{e}^T \boldsymbol{c}_{if}) = 0$
$-a_{\mathrm{in}}, \lambda_i, (\lambda_i \boldsymbol{e} + \boldsymbol{a}_{if}) > 0$

Therefore, this friction model has *Rolling, k (non-degenerate) sliding directions, separation,* and *approach* for possible contact modes resulting from the complementary cones of the LCP. We see that this friction model more accurately reflects out intuitive idea of an infinite number of sliding directions by discretizing the space into k-directions.

VII. Conclusion

This paper presents the equality of intuitive contact modes for rigid bodies with the cones generated from a linear complementarity formulation of the dynamics. Using multiple friction models, we represent the system as a linear complementarity problem and show how this formulation easily reduces to polyhedral convex cones. We analyzed these cones determining which were physically allowable, and showed the relationship with contact modes.

Acknowledgements

The authors wish to thank Devin Balkcom and Jong-Shi Pang for their technical guidance and suggestions. This paper was partially supported by NSF grant #0139701.

References

[1] J. Trinkle and J. J. Hunter, "A framework for planning dexterous manipulation," in *Proceedings, IEEE International Conference on Robotics and Automation*, April 1991, pp. 1245–1251.

[2] N. Zumel and M. Erdmann, "Nonprehensible two palm manipulation with non-equilbrium transitions between stable states," in *Proceedings, IEEE International Conference on Robotics and Automation*, April 1996, pp. 3317–3323.

[3] M. Cherif and K. Gupta, "Planning quasi-static fingertip manipulation for reconfiguring objects," *IEEE Transactions on Robotics and Automation*, vol. 15, no. 5, pp. 837–848, 1999.

[4] J. Pang and J. Trinkle, "Complementarity formulations and existence of solutions of dynamic multi-rigid-body contact problems with coulomb friction," *Mathematical Programming*, vol. 73, pp. 199–226, 1996.

[5] M. T. Mason and Y. Wang, "On the inconsistency of rigid-body frictional planar mechanics," in *Proceedings, IEEE International Conference on Robotics and Automation*, April 1988, pp. 524–528.

[6] D. Balkcom and J. Trinkle, "Computing wrench cones for planar rigid body contact tasks," *International Journal of Robotics Research*, vol. 21, no. 12, pp. 1053–1066, 2002.

[7] R. W. Cottle, J. Pang, and R. E. Stone, *The Linear Complementarity Problem*. Academic Press, 1992.

[8] D. Balkcom, E. Gottlieb, and J. Trinkle, "A sensorless insertion strategy for rigid planar parts," in *Proceedings, IEEE International Conference on Robotics and Automation*, 2002, pp. 882–887.

[9] M. T. Mason, *Mechanics of robotic manipulation*. MIT Press, 2001.

[10] A. J. Goldman and A. W. Tucker, "Polyhedral convex cones," in *Linear Inequalities and Related Systems*, H. W. Kuhn and A. W. Tucker, Eds. York: Princeton Univ., 1956, pp. 19–40.

[11] J. Trinkle, J. Pang, S. Sudarsky, and G. Lo, "On dynamic multi-rigid-body contact problems with coulomb friction," *Zeitschrift für Angewandte Mathematik und Mechanik*, vol. 77, no. 4, pp. 267–279, 1997.

[12] D. Stewart and J. Trinkle, "An implicit time-stepping scheme for rigid body dynamics with coulomb friction," in *Proceedings, IEEE International Conference on Robotics and Automation*, 2000, pp. 162–169.